Stretchable Supercapacitors Based on Carbon Nanotubes-Deposited Rubber Polymer Nanofibers Electrode with High Tolerance against Strain

Juyeon Yoon[1], Joonhyung Lee[2*], and Jaehyun Hur[1]*

[1]Department of Chemical and Biological Engineering, Gachon University, Seongnam, Gyeonggi 13120, Republic of Korea

[2]Device & System Research Center, Samsung Electronics, Suwon, Gyeonggi 443-803, Republic of Korea

---

*Corresponding author. Tel: +82-31-750-5593; Fax:+82-31-750-8839

E-mail address: joonhyung2009.lee@samsung.com, jhhur@gachon.ac.kr

Abstract

We report a new fabrication method for a fully stretchable supercapacitor based on single wall carbon nanotube (SWCNT)-coated electrospun rubber nanofibers as stretchable supercapacitor electrodes. The deposition conditions of SWCNT on hydrophobic rubber nanofibers are experimentally optimized to induce a uniform coating of SWCNT. For surfactant-assisted coating of SWCNT, both water contact angle and sheet resistance were the lowest compared to the cases with other surface treatment methods, indicating the most effective coating approach. The excellent electromechanical properties of this electrode under the stretching condition is demonstrated by the measurement of Young's modulus and normalized sheet resistance. This superb tolerance of the electrode with respect to stretching results from i) high aspect ratios of both nanofiber templates and the SWCNT conductors, ii) highly elastic nature of rubbery nanofiber, and iii) strong adherence of SWCNT-coated nanofiber on the elastic ecoflex substrate. Electrochemical and electromechanical measurements on the stretchable supercapacitor devices reveal that the volumetric capacitance (15.2 F cm^{-3} at 0.021 A cm^{-3}) of the unstretched state is maintained for strains of up to 40 %. At this level of strain, the capacitance after 1,000 charge/discharge cycles is not significantly reduced. The high stability of our stretchable device suggests potential future applications in various types of wearable energy storage devices.

Keywords: Supercapacitors, Stretchable, SBS nanofiber, Carbon nanotube, Electrospinning

1.Introduction

Stretchable electronics are a class of platform technologies employed in many multidisciplinary fields such as wearable devices, skin sensors, and bio-integrated devices [1,2] . They generally refer to elastic devices that can sustain their functionality while mechanical stretching is applied. Recently, various studies have been conducted on stretchable electronics including interconnect electrodes [3] , organic light emitting diode (OLEDs) [4] , pressure and strain sensors [5,6] , field effect transistors [7-10] , solar cells [11,12] , lithium ion batteries [13,14] , temperature sensors [15,16], electronic eyes [17], and electrochemical devices [18-27]. Among various energy-source devices, stretchable supercapacitors have emerged as one of the most indispensable components of stretchable electronics because of the high power delivered compared with other energy devices. Furthermore, a relatively simple fabrication process is another advantage in realizing the fully stretchable devices.

Despite these advantages, there are still some critical issues that have to be overcome to develop a high-performance and mechanically durable stretchable supercapacitors. First, the structure of electrode material as well as substrate should be highly tolerable against the strain. In resolving these issues, many different structures have been proposed including the wavy electrode materials on polymeric film substrates, coating active materials on textiles, and wrapping conductive materials on elastic polymeric fibers [28-31]. Second, the mechanical robustness and stability of other device components (separator and cell holder) upon stretching should be also guaranteed. Third, the fabrication of individual component and assembly process should be simple. Without satisfying these requirements, the stretchable supercapacitors cannot be properly operational under the harsh mechanical conditions such as stretching deformation.

To date, a variety of different methods have been demonstrated to fabricate stretchable supercapacitors. Single-walled carbon nanotubes (SWCNT) or graphenes deposited on buckled

rubber substrate have been used as electrodes for stretchable supercapacitors [28,32,33]. The coating of conductive ink such as SWCNT or polypyrrole on textile substrate, is another approach that has been used to realize stretchable supercapacitors [29]. Aboutalebi et al. fabricated graphene yarn electrodes that were employed to construct a stretchable energy storage device [34]. Similarly, elastic fiber coated with multiple layers of CNTs and electrolyte was demonstrated to be another type of stretchable supercapacitor [31]. Furthermore, a two-dimensional stretchable micro-supercapacitor was shown to be functional, which used a SWCNT pattern with ion-gel-type or horizontally aligned CNT and a polymeric-gel-type electrolyte on a transparent rubber substrate [35,36]. In spite of all of these studies, most of these approaches are limited by difficult fabrication processes or poor electromechanical performances, with the latter starting to degrade at relatively low strain.

Herein, we developed a highly stretchable supercapacitor based on SWCNT-deposited electrospun (e-spun) elastic rubber nanofiberous mats. Poly(styrene-b-butadiene-b-styrene) (SBS) was used as an e-spun nanofiber because of its great elasticity, while a highly stretchable silicone gel mixture (Ecoflex) was adopted as a substrate. Ecoflex has a Young's modulus of $\sim$ 60 kPa, far softer than that ($\sim$ 1.5 MPa) of commonly used polydimethylsiloxane (PDMS), affording much improved mechanical properties under stretching [37]. The SWCNTs were deposited on e-spun SBS via simple dipping and drying processes. Because this coating process was highly influenced by the surface properties of the SBS nanofibers, the most appropriate surface treatment was determined experimentally. A bare e-spun SBS nanofiberous mat immersed in ionic liquid was used as an elastic separator. Supercapacitors produced using our approaches are fully stretchable because all constituent components are durable and functional under stretching. The main advantages of our approaches are a remarkably simple fabrication process without the need of expensive equipment and excellent performances in terms of capacitance retention during the charge-discharge processes under the stretched state. The

facile fabrication and excellent performances of our devices meet all the requirements for stretchable supercapacitors mentioned earlier, thus present a promising stretchable energy storage device for various applications.

2. Experiments

2.1. Preparation of electrospun SBS nanofibrous mats

SBS solution (Aldrich, Mw = 140,000 g/mol, styrene = 30 wt.%) was prepared by dissolving SBS (10 wt.%) in a solvent mixture of tetrahydrofuran (THF)/ dimethylformamide (DMF) (3:1, w:w). SBS nanofibers were collected by electrospinning, with SBS solution fed at a rate of 50 μl/min under an applied voltage of 20 kV. Typically, a total volume of 20 ml of SBS solution was electrospun on either octadecyltrichorosilane (OTS)-treated Si wafers or disposable wipers (Kimberly-Clark Kimtech, 20 (l) × 30 (w) cm) attached on a custom-made cylindrical collector rotating at 500 rpm. In preparing the OTS-treated Si surface, Si wafers were first cleaned with piranha solution (H_2SO_4 (3): H_2O_2 (1), v:v at 80°C for 10 min) to remove any organic contaminants. The Si wafers were then dipped in OTS/toluene solution (0.5 wt. %) for 5 min. In this process, the trichlorosilane group of OTS reacted with hydroxyl groups on the Si substrate to form a self-assembled monolayer (SAM). To remove the residual OTS, the OTS-treated Si wafers were sonicated in chloroform for 5 min. The electrospun SBS nanofibrous mat was carefully peeled off from either OTS-treated Si wafers or Kimtech (if the thickness of SBS nanofibrous mat was too thin, or too much tension was applied during the peeling process, the SBS nanofibrous mat was torn off). The SBS nanofiber mat was cut into 2.0 cm (l) × 1.2 cm (w) pieces using scissors.

2.2. Deposition of SWCNT on SBS nanofibrous mats

A SWCNT (Hanwha Nanotech Corp., 100 S/cm) ink solution was prepared by dispersing 10 mg of as-purchased SWCNTs with 5 mg of sodium dodecylbenzene sulfonate (SDBS) in 10 ml of deionized (DI) water using a probe-type sonicator (950 W, Ningbo SCIENTZ Biotechnology) for 2 h. UV/ozone (UVO) surface treatment, polydopamine coating,

and fluorinated surfactant (Aldrich, Zonyl FS-300) treatment were carried out to make the SBS nanofibrous mats hydrophilic. For the UVO treatment, SBS nanofibrous mats were placed in a UVO chamber (Jelight 144AX) for 15 min. For the polydopamine coating, the SBS nanofibrous mats were dipped in the dopamine (Aldrich) solution (2 mg/mL of dopamine dissolved in 10 mM Tris-HCl (Aldrich, pH 8.5)) for 12 h at room temperature. The color of the SBS nanofibrous mats changed from white to dark brown, indicating the formation of polydopamine on the nanofiber surfaces. Lastly, for the fluorinated surfactant treatment, 0.1 wt.% of Zonyl FS-300 (Aldrich) was applied on the SBS nanofiber mat. Then, SBS nanofibrous mat was simply dipped into SWCNT/SDBS solution for 3 min, gently washed with DI water several times, and vacuum dried at room temperature.

2.3. Assembly of a supercapacitor cell

The supercapacitor was assembled as a two-electrode system, with 1-Ethyl-3-methylimidazolium bis(trifluoromethylsulfonyl)imide (C-TRI, [EMIM][NTf2]) as the electrolyte. Ecoflex rubber film (Smooth-on, Supersoft 0010) was prepared by mixing rubber and curing agent (1:1, v:v) and casting it with a thickness of 1 mm. The cured Ecoflex film was cut into 2.5 cm (l) × 2.0 cm (w). Freestanding SWCNT-coated SBS nanofibrous mats were attached to the Ecoflex film by gentle pressing for complete adhesion. Owing to the highly tacky nature of the Ecoflex surface, the SWCNT-coated SBS nanofiber (SWCNT/SBS) mats attached firmly to the rubber surface and served both as porous electrodes and as current collectors. Separately, SBS nanofibrous mats (2.2 cm (l) x 1.5 cm (w)) immersed in [EMIM][NTf2] were used as separators between pairs of identical Ecoflex/SWCNT-coated SBS nanofibrous mat electrodes. To ensure good electrical contacts, a copper strip was attached to the edge of each SWCNT-coated SBS fiber mat and a clip was placed in the middle of each cell. The assembled supercapacitors were mounted on a custom-made sample stage for

electrochemical and stretching experiments.

2.4. Measurement of electrochemical performances

Electrochemical measurements on the stretchable supercapacitors were carried out on a custom-made sample stage. Cyclic voltammetry (CV) and galvanostatic charge-discharge (GCD) measurements were performed using a Bio-Logic VSP potentiostat/galvanostat in a voltage window of 0.0 to 3.0 V with sweep rates of 5–100 mV s^{-1} for CV and current densities of 0.021–0.208 A cm^{-3} for galvanostatic measurements. For two-electrode configuration, the volumetric capacitance (C_v) was calculated from the CV or GCD discharge curve using the following equation, [19]

$$C_v = \int_a^b \frac{I(E)}{vV(b-a)} dE \quad \text{(from CV curve)} \tag{1}$$

where I(E), υ, V, a, and b refer to the measured current, the scan rate, the volume of the two electrodes, the starting and the ending voltage of the CV measurement, respectively, and

$$C_v = \frac{2I}{V(\frac{\Delta E}{\Delta t})} \quad \text{(from GCD curve)} \tag{2}$$

where I, V, ΔE, and Δt denote the applied current, the volume of the two electrodes, the applied voltage, and the discharge time after IR drop, respectively. The long-term cycling test was performed at 0.083 A cm^{-3} with a cutoff potential of 3.0 V.

2.5. Characterization

The morphology of the SWCNT-coated SBS nanofibers was observed by field-emission scanning electron microscopy (FESEM, JSM 7000F, JEOL). The sheet resistance of the SWCNT-coated SBS nanofibrous mats was measured using a four-point probe with a linear probe head (1.0 mm gap, Jandel HM21, UK). The contact angle of a water droplet on the electrode was measured using a drop-shape analysis system (DSA10-MK2, Krüss, Germany). The mechanical property of the electrospun film was measured using a uniaxial tensile test

(Lloyd Instruments).

3. Results and Discussion

3.1. Preparation of stretchable supercapacitors

Fig. 1 presents a schematic diagram of the methodology for fabricating stretchable supercapacitors. In order to make a nonwoven mat of SBS nanofibers, a sufficient amount of SBS (~ 2 g) was electrospun on the collector.
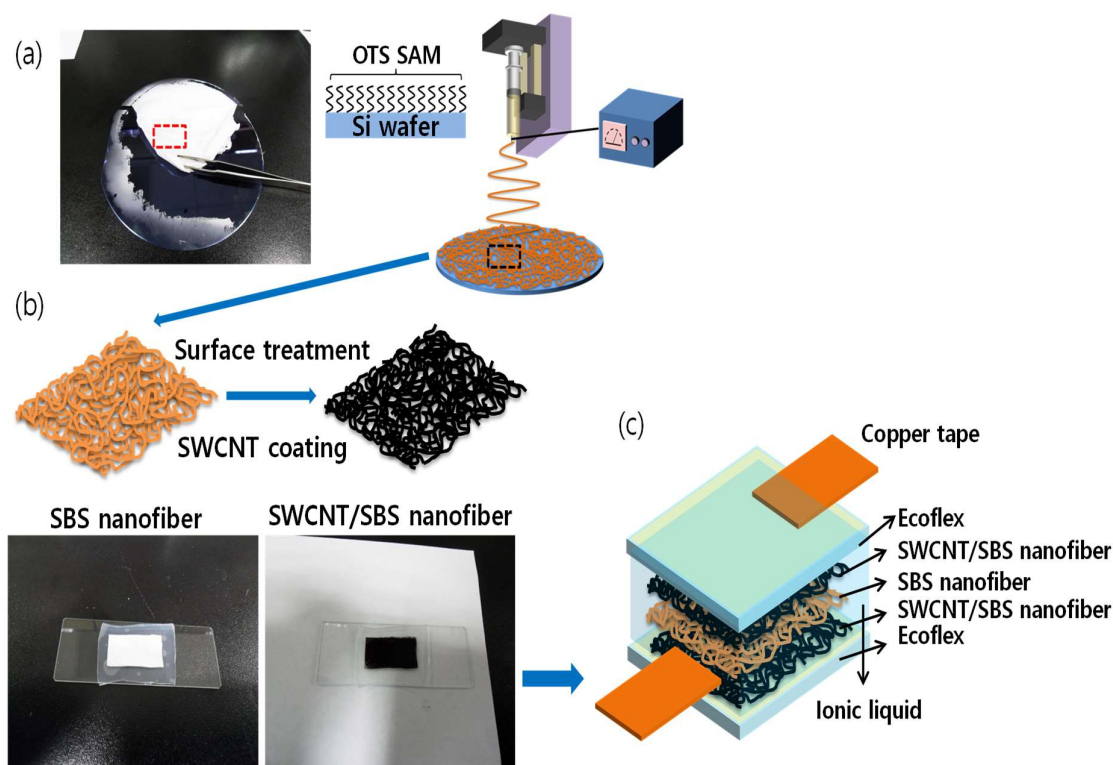

Fig. 1. Schematic description of the stretchable supercapacitor fabrication process. (a) Electrospinning of SBS on the OTS SAM-treated silicon wafer, (b) SWCNT coating on SBS nanofibrous mat/Ecoflex after surface treatment (Photographs of SBS nanofiber mat and SWCNT/SBS stretchable electrode were presented below), (c) Assembled stretchable supercapacitor device.

As more SBS nanofibers accumulated, the mechanical strength (i.e., tolerance with respect to breakage) increased, but the effective elasticity of the freestanding film decreased. The current collectors used in our experiment were either OTS SAM-treated silicon wafers or commercially available disposable wipers. Their highly hydrophobic surface allowed the nonwoven mat of SBS nanofibers to be peeled off easily (Fig. 1a) without any damage and used as freestanding films. The variations in thickness of the detached nanofiber mats were within 10 % of the average thickness (typically ~100 μm). SWCNT were coated on the SBS nanofibers using a simple dipping and drying process (Fig. 1b). The freestanding SWCNT/SBS films were attached on Ecoflex rubber. The sticky surface of Ecoflex allowed strong adhesion to the films without the need of any adhesives or additional binder. Additional freestanding film of SBS nanofiber was used as a stretchable separator. Supercapacitor cells were prepared by sandwiching a SBS nanofiber mat separator immersed in an ionic liquid ([EMIM][NTf2]), between two SWCNT/SBS electrodes attached on Ecoflex substrates (Fig. 1c).

3.2. Effect of SBS nanofiber surface treatment on the SWCNT coating

The morphologies of the SWCNT-coated SBS nanofibrous mats were examined upon applying different surface treatments on the SBS nanofibrous mats. Normally, aqueous SWCNT solutions dispersed with a surfactant (SDBS) hardly wet the SBS nanofiber surface because of the strong intrinsic hydrophobic property of SBS. Moreover, the rugged surface of the SBS nanofibers further increases its hydrophobicity. Consequently, in order to coat the SWCNTs, the wettability should be improved by an appropriate surface treatment that can increase the surface energy of the SBS nanofibrous mats. Fig. 2 compares the morphologies of SWCNT/SBS nanofibrous mats after three different treatments for the SBS nanofiber surface, namely UVO treatment, polydopamine coating, and fluorinated surfactant (Zonyl) treatment.

It has been known that these are widely used techniques to improve surface wettability, leading to enhanced adhesion. Following UVO treatment, the SWCNT did not uniformly adhere to the SBS nanofiber surface (see Figs. 2a and 2d, and the inset of Fig. 2a).
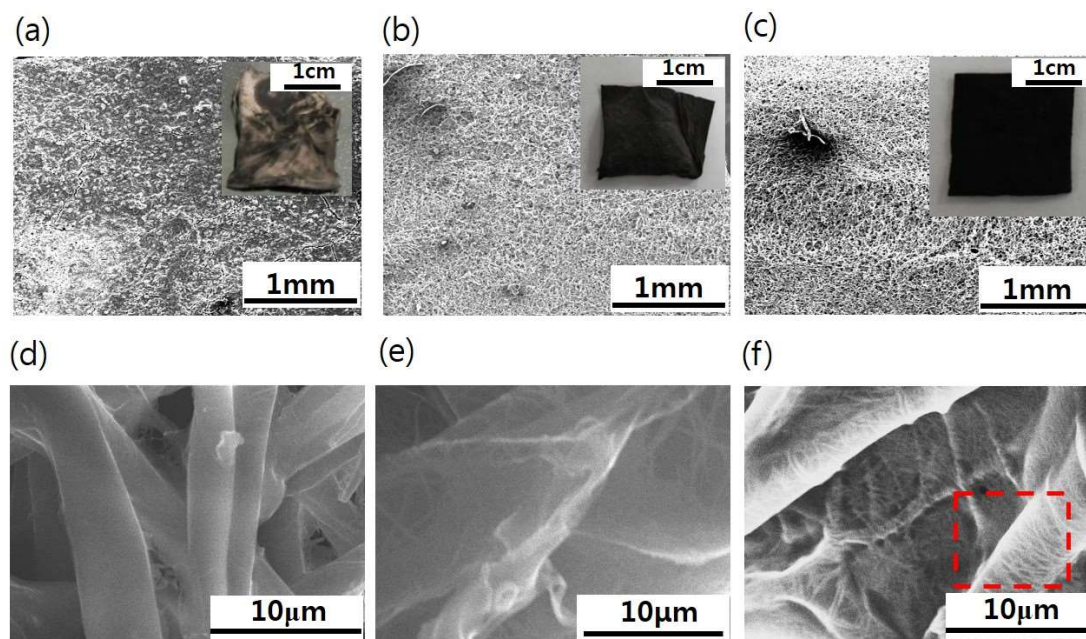

Fig. 2. Field-emission scanning electron micrographs (FESEM) of the SWCNT/SBS nanofiber mats following different surface treatments: (a and d) UVO treatment, (b and e) Polydopamine treatment, (c and f) Zonyl treatment. The insets in (a – c) show photographs of the SWCNT/SBS nanofiber mats. The red dotted box in Fig. 2f clearly shows the densely coated SWCNT on SBS nanofiber.

This is a consequence of the rugged surface of the SBS nanofibrous mats, which does not allow UVO to reach all surfaces within the three-dimensional fibrous matrix. For the polydopamine coating, the nanofiber films were simply immersed in the dopamine solution under basic conditions, resulting in polydopamine formation on the surface of the fibers. [38] However, in this case, although the uniformity of the SWCNT coating was much improved compared with UVO treatment, the resulting SWCNT density was still insufficient, as revealed

in Figs. 2b and 2e. Lastly, the nanofiber surfaces were treated with a fluorinated surfactant by coating Zonyl onto SBS nanofibers. Zonyl-treated freestanding SBS nanofiber film was dipped in the SWCNT solution to coat the SWCNT. The change in wetting behavior of SWCNT for Zonyl-treated SBS nanofiber was remarkably different from untreated SBS nanofibrous mat. Indeed, the improvement of coating behavior in the presence of Zonyl is evident with the micrograph shown in Figs 2c and 2f, where the density of SWCNT on the SBS nanofibers is by far greater than cases in UVO (Fig. 2d) and polydopamine treatments (Fig. 2e).

3.3. Wetting, mechanical and electrical characteristics of SWCNT/SBS nanofibrous mats following different surface treatments

The characteristics of SWCNT/SBS nanofibrous mats after the different surface treatments were more quantitatively analyzed by measuring their wetting and electrical properties. Figs. 3a and 3b reveal the contact angle and sheet resistance of SWCNT/SBS after three different treatments (UVO, polydopamine, and Zonly).
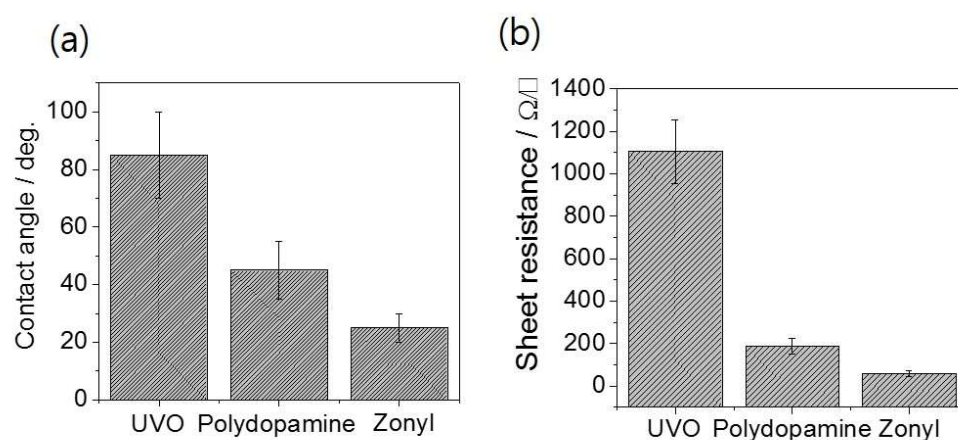

Fig. 3. (a) Contact angle of the water droplet on the SBS nanofiber film after different surface treatments (UVO, Polydopamine, Zonyl), (b) Sheet resistance following three different surface treatments.

The contact angle (25° ± 5°) of Zonly-treated surface was much smaller than other surface treatment methods (85° ± 15° and 45° ± 10° and for UVO and polydopamine treatment, respectively, Fig. 3a), which was consistent results observed in both photographs and SEM images. From the sheet resistance measurements, they were measured to be 1105 ± 151, 187 ± 38, and 58 ± 15 $\Omega/\square$ for the SWCNT/SBS following UVO, polydopamine, and Zonyl treatments, respectively (Fig. 3b). Here, it is of note that the thickness and surface area of SBS nanofiber mats were fixed as ~ 100 μm and 2.2 cm (l) × 1.5 (w) cm, and that the substrate dipping conditions were identical.

For the best sample (Zonyl-treated SWCNT/SBS), the mechanical property of the nanofiber film was measured using a uniaxial tensile test (Fig. 4a). For SBS nanofiber film, the Young's modulus was measured to be ~ 0.94 MPa. On the other hand, the Young's modulus of SWCNT-coated SBS nanofiber film was ~ 4.22 MPa, indicating the much rigid film after SWCNT coating. For both cases, there were strain values at which Young's modulus suddenly changes; these were ~ 45 % and ~ 80 % of strain for SBS and SWCNT/SBS, respectively. After these points, the nanofiber films undergo the irreversible deformation; thus suggesting the maximum tolerable strain for each case. Fig. 4b presents the normalized resistance ($\eta = R/R_o$, where R_o and R refer to the sheet resistance of SWCNT/SBS sheet before and after stretching, respectively) as a function of the applied strain. For a stretched SWCNT/SBS, the normalized resistance with respect to unstretched state remained almost invariant up to ~ 45 % strain, which is coincident with our previous tensile test. Beyond this threshold value, the resistance increased radically, implying a breaking of most of the percolation network between the SWCNT. This point is higher than those (~ 30 %) reported in the literature where a buckled substrate was utilized in stretching experiments.[18,25]
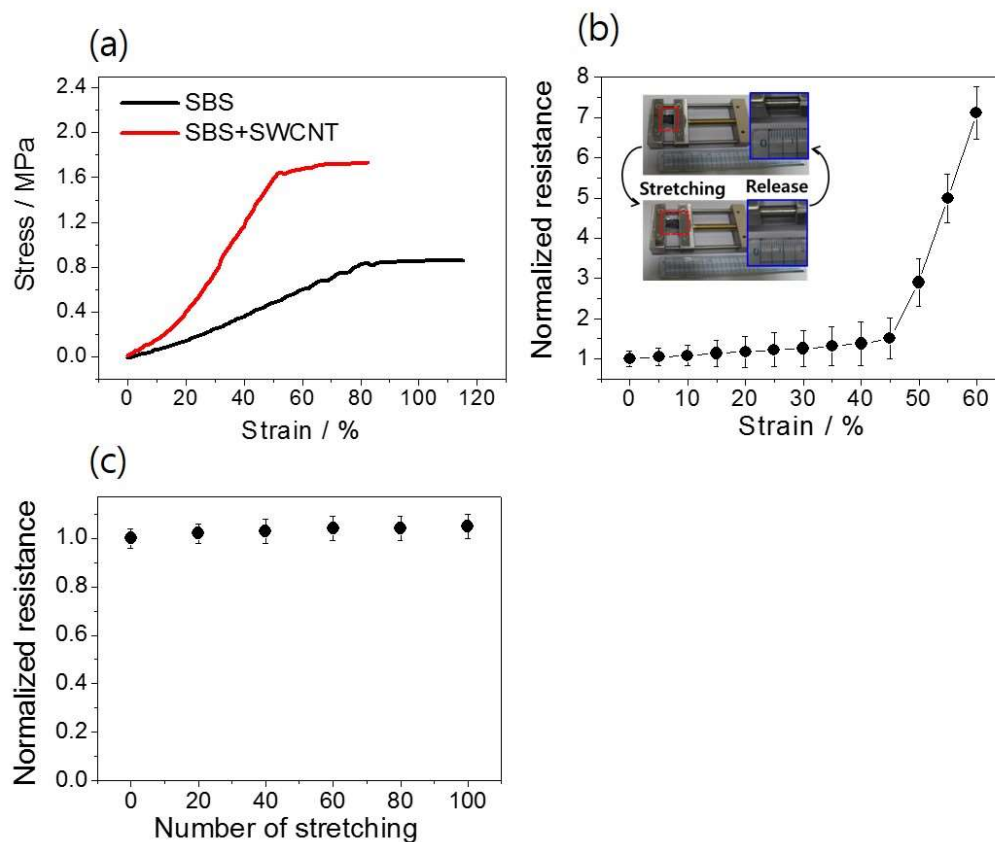
Fig. 4. Mechanical and electrical properties of the SWCNT/SBS nanofiber mat electrodes. (a) strain-stress curve for SBS and SWCNT-coated SBS nanofiber film, (b) Variation of the normalized sheet resistance as a function of the applied strain for Zonyl-treated SWCNT/SBS nanofiber mat electrodes; The inset shows the photograph of the stretching apparatus at different stages of the stretch/release cycle, (c) Normalized resistance as a function of the number of stretching cycles at 40% strain.

There are four advantages to our approach that contribute to this much increased threshold value of percolation break point. First, the entangled structure of the one-dimensional electrospun SBS nanofibers is already as tolerant to stretching as the previously used buckled substrates. [3,4] (Refer to Scheme 1) In other words, the one-dimensional form

factor of the SBS nanofibers that consists of the two-dimensional mat can better sustain elongational strain than its two-dimensional counterpart (i.e. SBS thin films). Indeed, this effect was directly confirmed by the observation of both SBS and SWCNT-SBS nanofibers before and after the stretching (Fig. S1). It was found that the applied strain induced only alignment of individual fibers without any damage because of the buckled structure of as-prepared nanofibers.
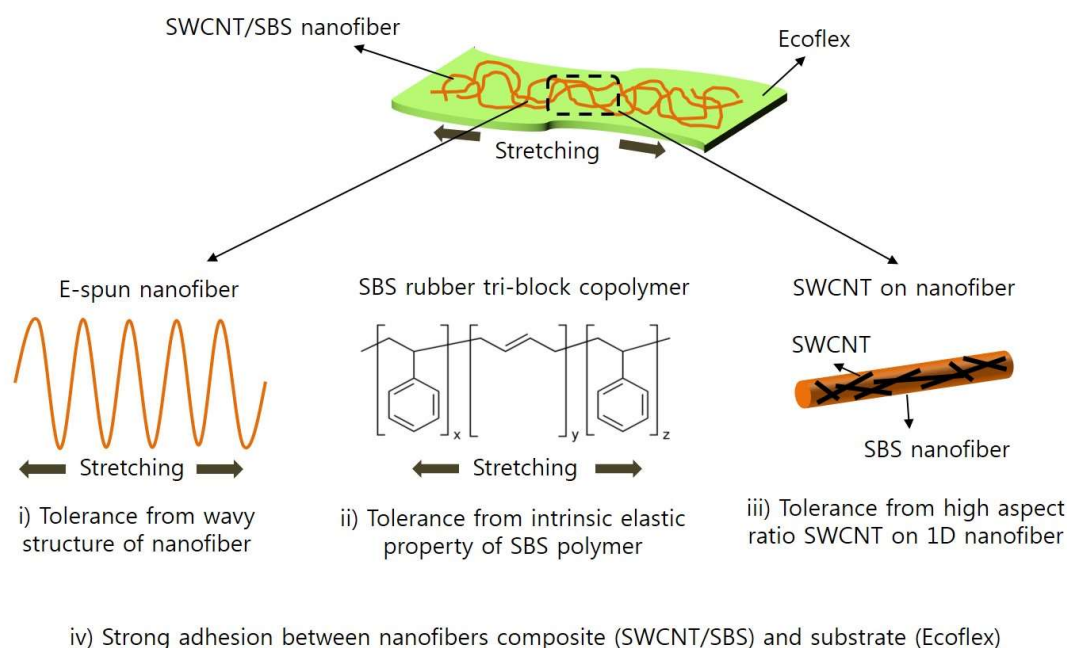
Scheme 1. Mechanism of high tolerance against strain for SWCNT/SBS nanofiber/Ecoflex stretchable electrode.

Second, an intrinsically high elasticity (i.g., Young's modulus ~ 0.94 MPa) [39] of electronspun SBS polymer significantly contributes to a high tolerance against mechanical stretching. Third, the percolation network formed by multiple SWCNTs with a high aspect ratio deposited on the nanofiber effectively increases the stain at which the percolation network breakage takes place. Lastly, the strong adhesion between nanofiber composite (SWCNT/SBS) and Ecoflex substrate is another reason for the high endurance of the SWCNT/SBS streatchable electrode. Fig. 3c

displays the normalized resistance of SWCNT/SBS stretchable electrodes for multiple stretch/release deformations at 40% strain applied repeatedly. The normalized resistance increased less than 5% over the first 100 cycles of stretch/release, suggesting that three-dimensional SWCNT/SBS porous sheet electrode possesses high mechanical stability against strain. However, when the strain was greater than 50%, the normalized resistance increased irreversibly with the increased number of deformations. This resistance increase with repeated deformations is associated with a gradual rupturing of the percolation network that does not reform between cycles. Consequently, the stretching experiments were carried out mainly below 40 % strain.

3.4. Supercapacitor performances at different stretching ratios

Prior to the measurement at stretched state, we first evaluated the electrochemical performances of our supercapacitor with two-electrode configuration in the absence of stretching. Fig. 5a displays the CV curves of the devices at scan rates from 0.005 to 0.1 V s^{-1}. All the curves showed the symmetrical and rectangular shape irrespective of the scan rate, indicating that ions diffuse/accumulate effectively in the porous stretchable electrode. The calculated volumetric capacitances were 12.8, 9.8 5.6, and 4.3 F cm^{-3} at the scan rate of 0.005, 0.01, 0.05, and 0.1 V s^{-1} (Fig. 5b). Fig. 5c shows the GCD cuves within a potential window of 3.0 V at current density from 0.021 to 0.208 A cm^{-3}. Slight deviation from the linear relationship between potential and time was acquired at different current densities (Fig. 5c). This behavior is often observed in the symmetric supercapacitors rather than asymmetric counterparts [40,41]. It is reported to be because of the higher internal resistance in symmetric supercapacitors [40,42]. The high IR drop observed in our symmetric device could explain this non-linear behavior. The volumetric capacitance (calculated from the discharge time after IR drop at each current density) varied from 15.2 to 6.5 F cm^{-3} within the current densities applied above (Fig.
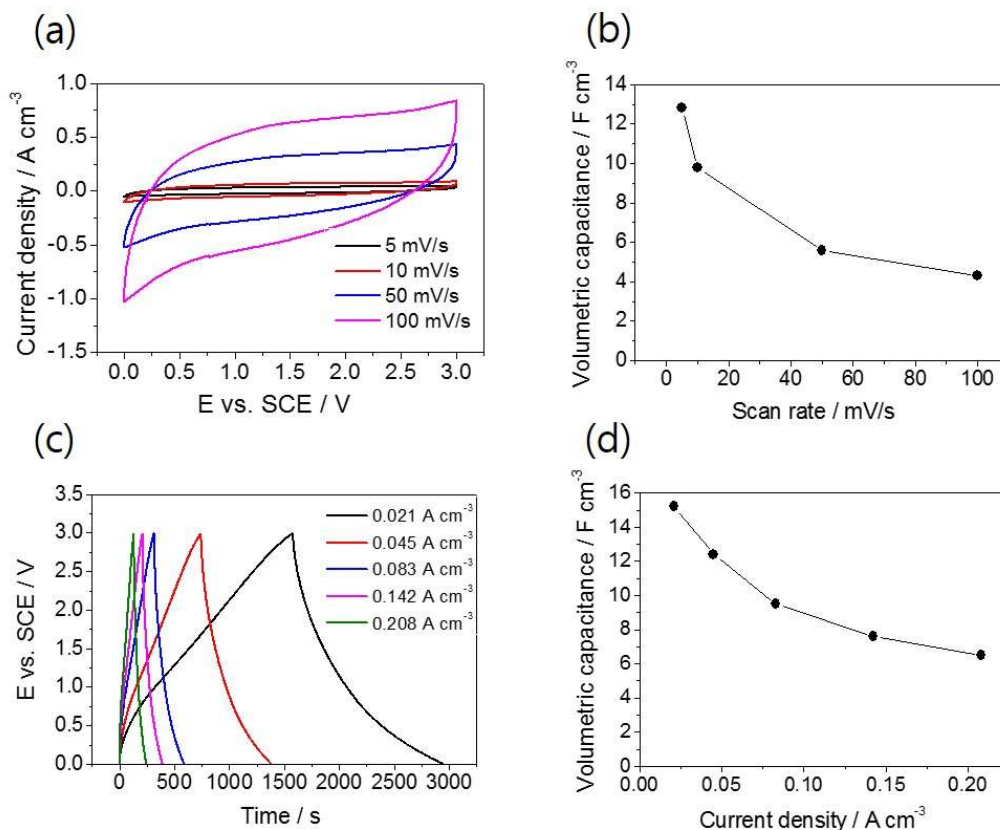
5d).

Fig. 5. Electrochemical measurements of the as-prepared stretchable supercapacitor. (a) Cyclic voltammograms of the supepcapacitor at a scan rate from 0.005 to 0.1 V s-1, (b) Volumetric capacitance as a function of scan rate, (c) Galvanostatic discharge curves at various current densities, (d) Volumetric capacitance as a function of current density.

Fig. 6 exhibits the various electrochemical performances upon applying different stain values. As shown in Fig. 6a, with stretching of up to 40 % strain, the CV curve approximately maintains its original shape, meaning that no significant irreversible change or damage took place even in liquid environment inside the device. These behaviors were consistently observed at different voltage scan rate upon 20 and 40% strain (Fig. S2). However, at a stretching ratio

of 50 %, the CV curve began to distort due to the irreversible deformation of the SWCNT/SBS

electrodes as consistent with the results of tensile test and sheet resistance measurements. The

volumetric capacitance value (C_v), calculated from GCD measurement (Fig. 6b), provided a

more quantitative comparison although the charge-discharge behavior was not perfectly linear

(the factors that can influence this non-linear behavior was already discussed earlier). For

tolerable stretching ratios (less than 40 %), the volumetric capacitances at a discharge current

density of 0.021 A cm^{-3} were measured to be 15.2, 14.8, and 14.5 F cm^{-3} for stretching ratios

of 0%, 20% and 40%, respectively (Fig. 6b and 6c). This suggests that our device is robust

even in a highly stretched state. The trend in volumetric capacitance variation as a function of

the discharge current density is also similar for unstretched and stretched supercapacitors (Fig.
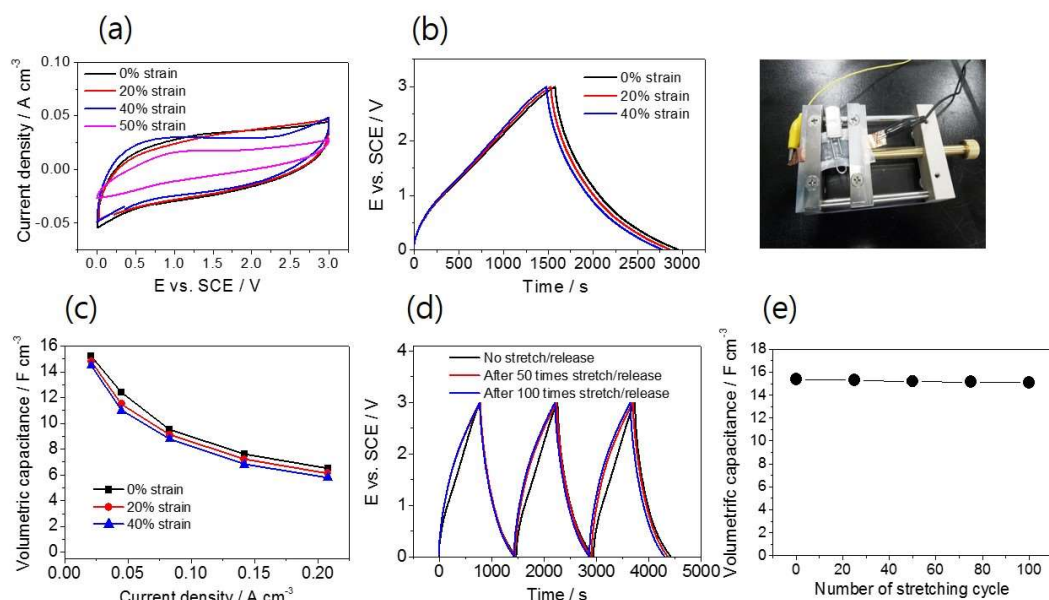
6c).

Fig. 6. Electrochemical performance of the supercapacitors upon stretching. (a) Cyclic

voltammograms for devices under 0 %, 20 %, and 40 %, and 50 % strain, (b) Galvanostatic

charge/discharge curves for a devices under 0 %, 20 %, and 40 % strain; and on the right, a

photograph taken during a stretching experiment, (c) Volumetric capacitance as a function of

discharge current density for devices under 0 %, 20 %, and 40 % strain, (d) Galvanostatic charge/discharge curves at a current density of 0.045 A cm^{-3} following 0, 50, and 100 times of repeated stretch/release cycles at 40 % strain, (e) Variation of volumetric capacitance after the different number (0, 25, 75, and 100) of stretch/release cycles.

The decrease in volumetric capacitance with increasing current density observed in both cases is commonly associated with ineffective ion accumulation/dissociation in porous SWCNT/SBS nanofiber mat electrodes. Nevertheless, it was remarkable that the functionality of device retained the good condition. For example, the difference in volumetric capacity between 0 % and 40 % strain was less than 1 %. Fig. 6d displays the charge/discharge curves measured after different number (0, 50, and 100) of repeated stretch/release cycles at a current density of 0.045 A cm^{-3} when 40 % of strain was applied. Here, it is of note that the first discharge time after IR drop was used to calculate the capacitance for different number of stretching (Fig. 6d). The capacitance drops after 50 and 100 times of stretch/release were also less than 1 % for both cases (Fig. 6e). This small level of performance deterioration after the harsh mechanical deformation clearly highlights a high robustness of our device.

The high mechanical stability of our stretchable device was also confirmed by long-term charge/discharge cycling measurements at a current density of 0.083 A cm^{-3} (Fig. 7a). Markedly, the capacitance after 1,000 charge-discharge cycles dropped only 2.6 %, 4.5 %, and 5.5 % for 0 %, 20 %, and 40 % strain, respectively. This trivial decrease in capacitance for the stretched state suggests that our device maintains a great level of performance under strains of up to 40 %. Even after 100 cycles of stretch/release deformation, although the initial capacity drop was observed compared to as-prepared SWCNT/SBS electrode, the degree of capacity fade (~ 7 %) during 1,000 cycles after 100 cycles of stretch/release was within the similar degree when compared with the case in 0 % strain (~ 3 %) without deformation. Additionally,

the volumetric power and energy densities in the SWCNT/SBS nanofiber supercapacitors were calculated from the GCD curves (data measured in Fig. 5c and 5d, namely, 15.2, 12.4, 9.5, 7.6, and 6.5 F cm^{-3} without stretching) using the relationships, E_v (mWh cm^{-3}) = 0.5C$_v$ $\Delta E^2 \times (1000/3600)$ and P (mW cm^{-3}) = 3600 E_v/t, where C_v, ΔE, and t denote the calculated volumetric capacitance, potential, and time after IR drop, respectively (Fig. 7b). An volumetric energy density of 2 - 5.6 mWh cm^{-3} and a volumetric power density of 158 - 1450 mW cm^{-3} were obtained for current densities of 0.021 - 0.208 A cm^{-3} in the SWCNT/SBS nanofibers. Comparing with previous works (Table S1) related to the various stretchable supercapacitors, the performances of our device is excellent and superior to the characteristics of currently available various commercial devices (Fig. 7b).
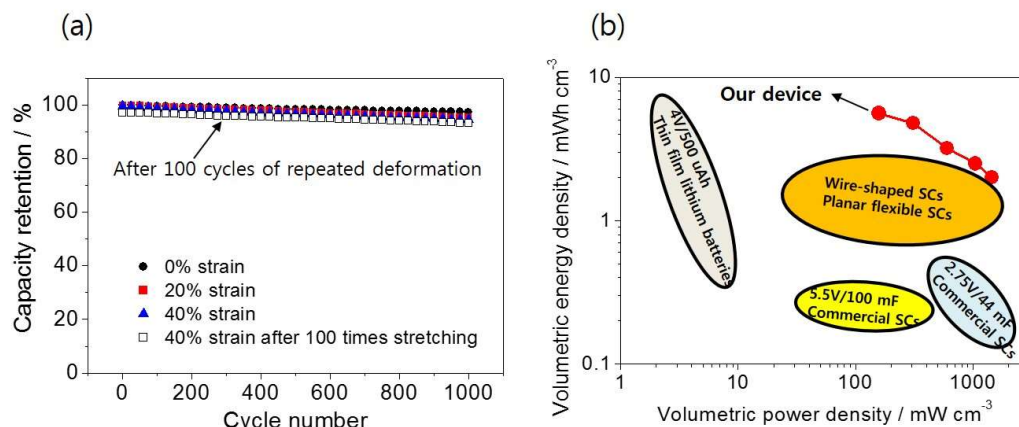

Fig. 7. Long-term cycling life (without and with stretching) and Ragone plot. (a) Capacitance retention as a function of the number of charge/discharge cycles at a current density of 0.083 A cm^{-3}, b) Ragone plots (volumetric energy density vs. volumetric power density) calculated from the galvanostatic charge/discharge curves at various current densities (from 0.021 to 0.208 A cm^{-3}).

4. Conclusion

In summary, a new and facile method for fabricating stretchable supercapacitor device

was developed using SWCNT/SBS nanofibrous mats on Ecoflex as stretchable electrodes, SBS nanofiber as a separator, and ionic liquid as an electrolyte. Fluorinated surfactant (Zonyl) treatment allowed the most uniform and effective coating of SWCNT on the SBS nanofibers. Breakage of the percolation network and the conductive pathways in our stretchable electrodes occurred only at ~ 45 % of strain, which were consistently confirmed by the mechanical and electrical analyses. Consequently, supercapacitors using our stretchable electrodes maintain their original performances (capacity retention of 93 %) even at a highly applied strain (40%) after 100 times of repeated stretching/release. The mechanical robustness and excellent electrochemical performances under repeated stretching are associated with the synergetic effects of structural features of constituents (i.e., wavy structure of e-spun rubber nanofibers as well as high aspect ratios of both SWCNT and e-spun fibers), the highly elastic nature (~0.94 MPa) of SBS rubber fibers, and strong adhesion between stretchable SWCNT-SBS fibrous mat and Ecoflex substrate. These results suggest our supercapacitors can provide excellent platform technology for various wearable energy storage devices, thanks to a simple and inexpensive fabrication process.

References

1.   Mohammed, M.G.; Kramer, R. All-printed flexible and stretchable electronics. *Adv. Mater.* **2017**, *29*, 1604965.

2.   Rogers, J.A.; Someya, T.; Huang, Y. Materials and mechanics for stretchable electronics. *Science* **2010**, *327*, 1603-1607.

3.   Ko, E.-H.; Kim, H.-J.; Lee, S.-M.; Kim, T.-W.; Kim, H.-K. Stretchable ag electrodes with mechanically tunable optical transmittance on wavy-patterned pdms substrates. *Sci. Rep.* **2017**, *7*, 46739.

4.   Yu, Z.; Niu, X.; Liu, Z.; Pei, Q. Intrinsically stretchable polymer light-emitting devices using carbon nanotube-polymer composite electrodes. *Adv. Mater.* **2011**, *23*, 3989-3994.

5.   Kim, T.-H.; Lee, C.-S.; Kim, S.; Hur, J.; Lee, S.; Shin, K.W.; Yoon, Y.-Z.; Choi, M.K.; Yang, J.; Kim, D.-H.*, et al.* Fully stretchable optoelectronic sensors based on colloidal quantum dots for sensing photoplethysmographic signals. *ACS Nano* **2017**, *11*, 5992-6003.

6.   Zhou, J.; Yu, H.; Xu, X.; Han, F.; Lubineau, G. Ultrasensitive, stretchable strain sensors based on fragmented carbon nanotube papers. *ACS Appl. Mater. Interfaces* **2017**, *9*, 4835-4842.

7.   Lu, C.; Lee, W.-Y.; Shih, C.-C.; Wen, M.-Y.; Chen, W.-C. Stretchable polymer dielectrics for low-voltage-driven field-effect transistors. *ACS Appl. Mater. Interfaces* **2017**, *9*, 25522-25532.

8.   Wen, H.-F.; Wu, H.-C.; Aimi, J.; Hung, C.-C.; Chiang, Y.-C.; Kuo, C.-C.; Chen, W.-C. Soft poly(butyl acrylate) side chains toward intrinsically stretchable polymeric semiconductors for field-effect transistor applications. *Macromolecules* **2017**, *50*, 4982-4992.

9.   Chae, S.H.; Yu, W.J.; Bae, J.J.; Duong, D.L.; Perello, D.; Jeong, H.Y.; Ta, Q.H.; Ly, T.H.; Vu, Q.A.; Yun, M.*, et al.* Transferred wrinkled al2o3 for highly stretchable and transparent graphene–carbon nanotube transistors. *Nat. Mater.* **2013**, *12*, 403.

10.   Kim, D.-H.; Ahn, J.-H.; Choi, W.M.; Kim, H.-S.; Kim, T.-H.; Song, J.; Huang, Y.Y.; Liu, Z.; Lu, C.; Rogers, J.A. Stretchable and foldable silicon integrated circuits. *Science* **2008**, *320*, 507-511.

11.   Lee, J.; Wu, J.; Shi, M.; Yoon, J.; Park, S.-I.; Li, M.; Liu, Z.; Huang, Y.; Rogers, J.A.

Stretchable solar cells: Stretchable gaas photovoltaics with designs that enable high areal coverage *Adv. Mater.* **2011**, *23*, 919-919.

12. Lipomi, D.J.; Tee, B.C.K.; Vosgueritchian, M.; Bao, Z. Stretchable organic solar cells. *Adv. Mater.* **2011**, *23*, 1771-1775.

13. Liu, W.; Chen, J.; Chen, Z.; Liu, K.; Zhou, G.; Sun, Y.; Song, M.-S.; Bao, Z.; Cui, Y. Stretchable lithium-ion batteries enabled by device-scaled wavy structure and elastic-sticky separator. *Adv. Energy Mater.* **2017**, *7*, 1701076.

14. Liu, W.; Chen, Z.; Zhou, G.; Sun, Y.; Lee, H.R.; Liu, C.; Yao, H.; Bao, Z.; Cui, Y. 3d porous sponge-inspired electrode for stretchable lithium-ion batteries. *Adv. Mater.* **2016**, *28*, 3578-3583.

15. Hong, S.Y.; Lee, Y.H.; Park, H.; Jin, S.W.; Jeong, Y.R.; Yun, J.; You, I.; Zi, G.; Ha, J.S. Stretchable active matrix temperature sensor array of polyaniline nanofibers for electronic skin. *Adv. Mater.* **2016**, *28*, 930-935.

16. Trung, T.Q.; Ramasundaram, S.; Hwang, B.-U.; Lee, N.-E. An all-elastomeric transparent and stretchable temperature sensor for body-attachable wearable electronics. *Adv. Mater.* **2016**, *28*, 502-509.

17. Ko, H.C.; Stoykovich, M.P.; Song, J.; Malyarchuk, V.; Choi, W.M.; Yu, C.-J.; Geddes Iii, J.B.; Xiao, J.; Wang, S.; Huang, Y*., et al.* A hemispherical electronic eye camera based on compressible silicon optoelectronics. *Nature* **2008**, *454*, 748.

18. Wang, S.; Liu, N.; Su, J.; Li, L.; Long, F.; Zou, Z.; Jiang, X.; Gao, Y. Highly stretchable and self-healable supercapacitor with reduced graphene oxide based fiber springs. *ACS Nano* **2017**, *11*, 2066-2074.

19. Shi, M.; Yang, C.; Song, X.; Liu, J.; Zhao, L.; Zhang, P.; Gao, L. Stretchable wire-shaped supercapacitors with high energy density for size-adjustable wearable electronics. *Chem. Eng. J.* **2017**, *322*, 538-545.

20. Xu, J.; Ding, J.; Zhou, X.; Zhang, Y.; Zhu, W.; Liu, Z.; Ge, S.; Yuan, N.; Fang, S.; Baughman, R.H. Enhanced rate performance of flexible and stretchable linear supercapacitors based on polyaniline@au@carbon nanotube with ultrafast axial electron transport. *J. Power Sources* **2017**, *340*, 302-308.

21. Lv, T.; Yao, Y.; Li, N.; Chen, T. Highly stretchable supercapacitors based on aligned carbon nanotube/molybdenum disulfide composites. *Angew. Chem.* **2016**, *55*, 9191-9195.

22. Lamberti, A.; Clerici, F.; Fontana, M.; Scaltrito, L. A highly stretchable supercapacitor

using laser-induced graphene electrodes onto elastomeric substrate. *Adv. Energy Mater.* **2016**, *6*, 1600050.

23.   He, S.; Cao, J.; Xie, S.; Deng, J.; Gao, Q.; Qiu, L.; Zhang, J.; Wang, L.; Hu, Y.; Peng, H. Stretchable supercapacitor based on a cellular structure. *J. Mater. Chem. A* **2016**, *4*, 10124-10129.

24.   Li, F.; Chen, J.; Wang, X.; Xue, M.; Chen, G.F. Stretchable supercapacitor with adjustable volumetric capacitance based on 3d interdigital electrodes. *Adv. Funct. Mater.* **2015**, *25*, 4601-4606.

25.   Tang, Q.; Chen, M.; Wang, G.; Bao, H.; Saha, P. A facile prestrain-stick-release assembly of stretchable supercapacitors based on highly stretchable and sticky hydrogel electrolyte. *J. Power Sources* **2015**, *284*, 400-408.

26.   Huang, Y.; Zhong, M.; Huang, Y.; Zhu, M.; Pei, Z.; Wang, Z.; Xue, Q.; Xie, X.; Zhi, C. A self-healable and highly stretchable supercapacitor based on a dual crosslinked polyelectrolyte. *Nat. Commun.* **2015**, *6*, 10310.

27.   Song, Z.; Wang, X.; Lv, C.; An, Y.; Liang, M.; Ma, T.; He, D.; Zheng, Y.-J.; Huang, S.-Q.; Yu, H*., et al.* Kirigami-based stretchable lithium-ion batteries. *Sci. Rep.* **2015**, *5*, 10988.

28.   Yu, C.; Masarapu, C.; Rong, J.; Wei, B.; Jiang, H. Stretchable supercapacitors based on buckled single-walled carbon-nanotube macrofilms. *Adv. Mater.* **2009**, *21*, 4793-4797.

29.   Hu, L.; Pasta, M.; La Mantia, F.; Cui, L.; Jeong, S.; Deshazer, H.D.; Choi, J.W.; Han, S.M.; Cui, Y. Stretchable, porous, and conductive energy textiles. *Nano Lett.* **2010**, *10*, 708-714.

30.   Huang, Y.; Tao, J.; Meng, W.; Zhu, M.; Huang, Y.; Fu, Y.; Gao, Y.; Zhi, C. Super-high rate stretchable polypyrrole-based supercapacitors with excellent cycling stability. *NANO ENERGY* **2015**, *11*, 518-525.

31.   Yang, Z.; Deng, J.; Chen, X.; Ren, J.; Peng, H. A highly stretchable, fiber-shaped supercapacitor. *Angew. Chem.* **2013**, *52*, 13453-13457.

32.   Li, X.; Gu, T.; Wei, B. Dynamic and galvanic stability of stretchable supercapacitors. *Nano Lett.* **2012**, *12*, 6366-6371.

33.   Chen, T.; Xue, Y.; Roy, A.K.; Dai, L. Transparent and stretchable high-performance supercapacitors based on wrinkled graphene electrodes. *ACS Nano* **2014**, *8*, 1039-1046.

34.   Aboutalebi, S.H.; Jalili, R.; Esrafilzadeh, D.; Salari, M.; Gholamvand, Z.; Aminorroaya Yamini, S.; Konstantinov, K.; Shepherd, R.L.; Chen, J.; Moulton, S.E*., et al.* High-performance multifunctional graphene yarns: Toward wearable all-carbon energy storage textiles. *ACS Nano* **2014**, *8*, 2456-2466.

35.   Kim, D.; Shin, G.; Kang, Y.J.; Kim, W.; Ha, J.S. Fabrication of a stretchable solid-state micro-supercapacitor array. *ACS Nano* **2013**, *7*, 7975-7982.

36.   Chen, T.; Peng, H.; Durstock, M.; Dai, L. High-performance transparent and stretchable all-solid supercapacitors based on highly aligned carbon nanotube sheets. *Sci. Rep.* **2014**, *4*, 3612.

37.   Marchal, M.; Allard, J.; Duriez, C.; Cotin, S. Towards a framework for assessing deformable models in medical simulation. In *Biomedical simulation: 4th international symposium, isbms 2008, london, uk, july 7-8, 2008 proceedings*, Bello, F.; Edwards, P.J.E., Eds. Springer Berlin Heidelberg: Berlin, Heidelberg, 2008; pp 176-184.

38.   Lee, H.; Dellatore, S.M.; Miller, W.M.; Messersmith, P.B. Mussel-inspired surface chemistry for multifunctional coatings. *Science* **2007**, *318*, 426-430.

39.   Luis, I.; David, P. Mechanical properties of thermoplastic butadiene–styrene (sbs) and oxidized short carbon fibre composites. *Polym. Int.* **1997**, *43*, 251-259.

40.   A., B.M.; G., A.G.; Teresita, K. Energy storage in symmetric and asymmetric supercapacitors based in carbon cloth/polyaniline–carbon black nanocomposites. *Int. J. Energy Res.* **2015**, *39*, 2053-2061.

41.   Senthilkumar, S.T.; Selvan, R.K.; Ulaganathan, M.; Melo, J.S. Fabrication of bi2o3∥ac asymmetric supercapacitor with redox additive aqueous electrolyte and its improved electrochemical performances. *Electrochim. Acta* **2014**, *115*, 518-524.

42.   T. M. Koper, M. Non-linear phenomena in electrochemical systems. *J. Chem. Soc. Faraday Trans.* **1998**, *94*, 1369-1378.

Supplementary Materials

Stretchable Supercapacitors Based on Carbon Nanotubes-Deposited Rubber Polymer Nanofibers Electrode with High Tolerance against Strain

Juyeon Yoon[1], Joonhyung Lee[2]*, Jaehyun Hur[1]*

[1]Department of Chemical and Biological Engineering, Gachon University, Seongnam, Gyeonggi 13120, Republic of Korea

[2]Device & System Research Center, Samsung Electronics, Suwon, Gyeonggi 443-803, Republic of Korea

*Corresponding author. Tel: +82-31-750-5593; Fax:+82-31-750-8839

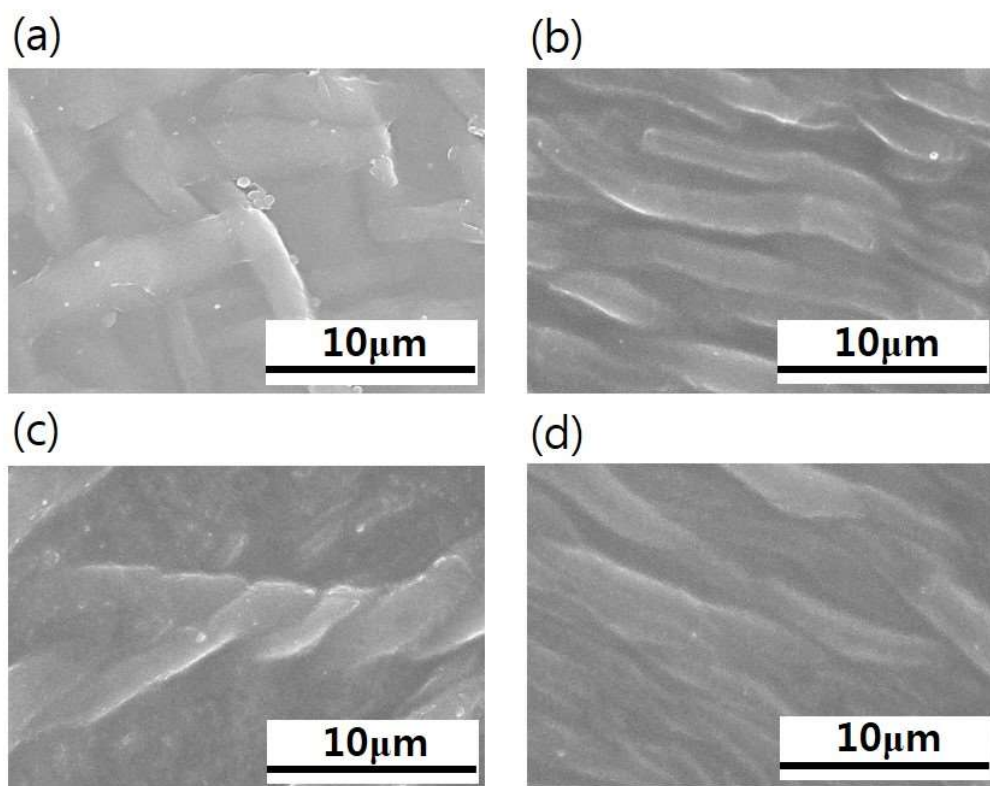E-mail address: joonhyung2009.lee@samsung.com, jhhur@gachon.ac.kr

Fig S1. Micrographs of SBS and SWCNT-SBS nanofibers before/after stretching: (a) SBS without stretching, (b) SBS with 40% strain, (c) SWCNT-SBS without stretching, and (d) SWCNT-SBS with 40% strain.
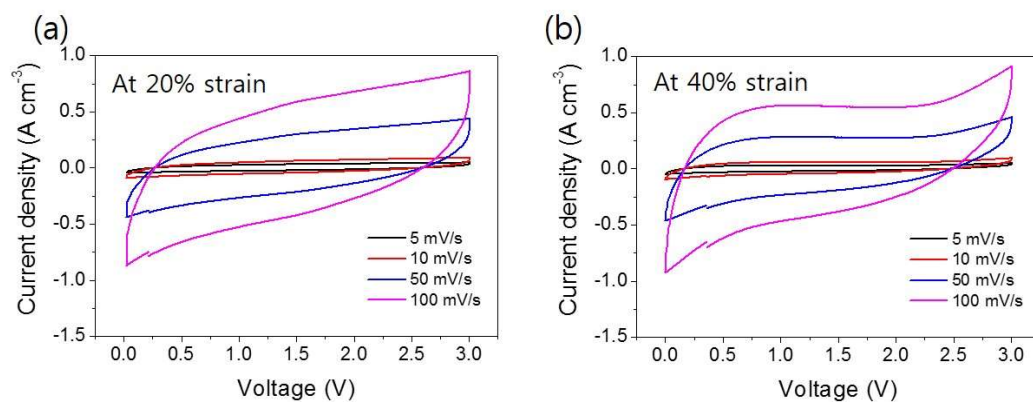
Fig. S2. Cyclic voltammograms of supercapacitors at the scan rate from 0.005 to 0.1 V s^{-1} upon

(a) 20%, and (b) 40% strain.

Electrode	Stretching ratio	Specific capacity (volumetric or areal or gravimetric)	Capacity retention under stretching	Power density (volumetric or gravimetric)	Energy density (volumetric or gravimetric)	Ref.
PPy/rGO/ MWCNT	100 %	10 F cm^{-3}	82.4 %	7.32 mW cm^{-3}	0.36-0.94 mWh cm^{-3}	18
CNT/Ag-coated yarn		5 F cm^{-3}		300-1000 mW cm^{-3}	2-5 mWh cm^{-3}	19
PANI@Au @CNT	400 %	6 F cm^{-3} (0.2 mF cm^{-2})	95 %			20
CNT/MoS$_2$ /PDMS	240 %	13 F cm^{-3}				21
Graphene/ PDMS	50 %	0.65 mF cm^{-2}				22
PANI/CNT	140 %	19 F cm^{-3} (72.9 mF cm^{-2})	98.3 %	337 mW cm^{-3}	0.7 mWh cm^{-3}	23
3D rGO	130 %	75 F cm^{-3} (120 F g^{-1})	97 %			24
CNT@MnO$_2$/hydrogel	150 %	6.6 mF cm^{-2}	90 %			25
PPy@CNT	600 %		350 %			26
Buckled SWNT	131.5 %	50 F g^{-1}	94.6 %			28
Buckled SWCNT	130 %	45 F g^{-1}	92.6 %			29
Wrinkled graphene	140 %	4.9 uF cm^{-2} (6.4 F g^{-1})				30

CNT/textile	120 %	800 mF cm^{-2} (62 F g^{-1})		30 kW kg^{-1}	20 Wh kg^{-1}	31
SWCNT-coated SBS nanofiber	145 %	15.2 F cm^{-3}	93 %	158-1450 mW cm^{-3}	2-5.6 mWh cm^{-3}	**This work**

Table S1. Comparison of the electrochemical performances for various stretchable supercapacitors from the previously researches with our work.